

Fluctuations of atomic energy levels due to axion dark matter

V. V. Flambaum* and I. B. Samsonov†

School of Physics, University of New South Wales, Sydney 2052, Australia

The amplitude of the pseudoscalar (axion) or scalar field fluctuates on a time scale of order of million field oscillation periods which is a typical coherence time in the virialized axion galactic dark matter halo model. This causes fluctuations of frequencies of atomic clocks on the same time scale. We show that this effect may be employed to search for the axion and scalar field dark matter with atomic and nuclear clocks. We re-purpose the results of the atomic clocks experiments comparing the variations of frequencies of hyperfine transitions in Rb and Cs atoms as well as in hydrogen atom vs cavity frequency fluctuations, and extract new limits on the axion coupling constant f_a for masses in the range 2×10^{-17} eV $\lesssim m \lesssim 10^{-13}$ eV. We also show that similar energy shifts arise in the second-order perturbation theory with linear in the pseudoscalar field interaction. These shifts may be potentially measured with nuclear clocks based on the low-energy transition in ^{229}Th nucleus. We propose a procedure which could, in principle, help determine the axion mass if the axion dark matter signal is present in experimental data sets.

I. INTRODUCTION

Scalar and pseudoscalar particles represent promising dark matter candidates which can fully saturate the local dark matter density $\rho_{\text{DM}} \approx 0.4 \text{ GeV/cm}^3$ [1–3]. If the mass of such a particle is low, $m \ll 1 \text{ eV}$, the number of such particles per De Broglie wavelength must be large, and the ensemble of these particles may be considered as a classical field oscillating harmonically in every particular point of space, $\phi = \phi_0 \cos(\omega t)$. The oscillation frequency ω is approximately equal to the dark matter particle mass m , $\omega \approx m$, since the kinetic energy is small, $E_k \sim 10^{-6}m$ (in this paper, we assume that the dark matter particles are virialized within the standard dark matter halo model, see, e.g., Refs. [4–6]). Interaction of the standard model particles (electron, photon, quarks, gluons) with this dark matter field produces oscillating shift of atomic energy levels which have been measured in a number of experiments, see, e.g., Refs. [7–17].

A general problem is that the mass of dark matter particle is unknown; therefore, one should do Fourier analysis of the data to separate the oscillating signal. However, if the interaction is proportional to the scalar field squared,

$$V = -g_f M_f \phi^2 \bar{\psi} \psi - \frac{g_\gamma}{4} \phi^2 F_{\mu\nu} F^{\mu\nu} + \dots, \quad (1)$$

the energy shift has a non-oscillating contribution owing to the identity

$$\phi^2 = \frac{1}{2} \phi_0^2 (1 + \cos(2\omega t)). \quad (2)$$

In Eq. (1), ψ is a Dirac fermion field with mass M_f , $F_{\mu\nu}$ is the Maxwell field strength, g_f and g_γ are the corresponding coupling constants. In general, the scalar field

may couple to other Standard Model fields, denoted by ellipsis in Eq. (1), which are not important in the present consideration.

Effects of quadratic-in- ϕ interaction in Eq. (1) may be described as an apparent variation of the fine structure constant, $\alpha' = \alpha(1+g_\gamma\phi^2)$, and masses of elementary particles, $M'_f = M_f(1+g_f\phi^2)$, see, e.g., Refs. [7, 8]. For example, the mass shift immediately follows from comparison of interaction with the scalar field $-g_f M_f \phi^2 \bar{\psi} \psi$ and fermion mass term in the Lagrangian $-M_f \psi \bar{\psi}$. Dependence of atomic transition frequencies on α , quark masses and ϕ^2 was studied in works [8, 9, 18–23]. Atomic spectroscopy methods have already allowed one to improve earlier cosmological limits on the interaction strength of low mass scalar field ϕ^2 with photons, electrons and quarks by 15 orders in magnitude [8, 9]. These limits have recently been revisited in Ref. [24] due to Big Bang Nucleosynthesis considerations. The experimental results were obtained by the measurements of oscillating frequency ratios of electron transitions in Dy/Cs [10], Rb/Cs [11], Yb/Cs [12], Sr/H/Si cavity [13], Cs/cavity [14], Yb/Yb/Sr [15, 16], where effects of the variation of frequencies may be interpreted as variation of α and fermion masses. In Ref. [25] it was proposed to search for the scalar field dark matter with interaction (1) by measuring fluctuations of the scalar field amplitude using magnetometer and optical atomic clock networks. In the case of linear-in- ϕ interaction, the use of a network of precision-measurement tools for searches of wave-like dark matter was proposed in Ref. [26].

The rest of this paper is organized as follows. In Sec. II we consider quadratic-in- ϕ atomic energy level corrections arising in the first order of perturbation theory and demonstrate that the mean value of these shifts should be (approximately) equal to the standard deviation due to the stochastic nature of the axion field amplitude. This relation allows us to find new lab-based limits on the axion decay constant f_a by re-purposing the results of the experiments [11] and [13], see Sec. III. Then, in Sec. IV we propose a procedure which, in principle, would allow one to identify the axion dark matter signal in experiments

* v.flambaum@unsw.edu.au

† igor.samsonov@unsw.edu.au

measuring fluctuations of energy level shifts with atomic clocks. This procedure utilizes the fact that the atomic energy levels fluctuations caused by axion dark matter should have a different statistical distribution from ordinary noise in the detector. In Sec. V we show that quadratic-in- ϕ contributions to the atomic energy level shifts appear also in the second order of perturbation theory. We compare these contributions to the corresponding first-order energy level corrections by considering the example of low-lying isomeric state in ^{229}Th nucleus. Section VI is devoted to a summary and discussion of the results of this paper.

We use natural units with $\hbar = c = 1$.

II. FIRST-ORDER PERTURBATION THEORY ENERGY LEVEL CORRECTIONS DUE TO QUADRATIC AXION-NUCLEON INTERACTION

In this section, we focus on the quadratic in the QCD axion field ϕ interaction with a nucleon as in Eq. (1). In Ref. [27] it was shown that this interaction originates from the standard QCD θ -term

$$\frac{g^2\theta}{32\pi^2}\tilde{G}^{l\mu\nu}G_{\mu\nu}^l, \quad (3)$$

with $\theta = \phi/f_a$, f_a is the axion decay constant, g is the strong interaction coupling constant, $G_{\mu\nu}^l$ is the gluon field strength and $\tilde{G}^{l\mu\nu}$ is its dual. Indeed, this axion-gluon interaction implies a variation of the pion mass [28],

$$\frac{\delta m_\pi}{m_\pi} \approx -0.05\theta^2. \quad (4)$$

This causes the corresponding variations of nuclear magnetic moment, nuclear mass and radius since these quantities depend on the pion mass, see Refs. [21, 29–32]. Variations of these quantities, in turn, lead to oscillations of atomic energy levels with angular frequency $2\omega \approx 2m$.

Let us assume that the experimental integration time t_1 significantly exceeds the oscillation period $T = \pi/m$, $t_1 \gg T$. In this case, the oscillating term in Eq. (2) averages to zero,

$$\overline{\cos(2\omega t)} = \frac{1}{t_1} \int_0^{t_1} \cos(2\omega t) dt = \frac{\sin(2\omega t_1)}{2\omega t_1} \rightarrow 0 \quad (5)$$

for $\omega t_1 \gg 1$, and the quadratic interaction (1) implies the following shift of an atomic energy level in the first order of perturbation theory

$$E \equiv \langle V \rangle = C(\phi_0)^2, \quad (6)$$

where C is a time-independent constant.

The problem is that only the time dependence of atomic energy shifts produced by new interactions can be measured accurately. Usually, the time-independent

contribution to the energy shift is hidden by uncertainties of theoretical values of energies in multielectron atoms.

In the case of quadratic interaction (1) with the scalar field (2) this problem may be addressed as follows. The amplitude of the scalar or pseudoscalar (axion) field ϕ_0 fluctuates on the time scale $\tau \sim 10^6 T$ (coherence time), see, e.g., Ref. [33]. This causes fluctuations of the energy shift (6) of atomic, molecular and nuclear transition energies. One can set the averaging time t_1 much smaller than coherence time τ but much larger than the oscillation period T ,

$$T \ll t_1 \ll \tau. \quad (7)$$

Repeating such measurements N times such that the total measurement time $t = Nt_1$ exceeds the coherence time τ , $t \gg \tau$, one can measure variance of fluctuations of the energy shift E

$$\sigma^2 = \overline{(E - \bar{E})^2} = \overline{(E^2)} - \overline{(E)}^2 = k(\bar{E})^2, \quad (8)$$

where the coefficient k is $O(1)$.

In Refs. [33, 34] it was shown that the amplitude of the scalar field ϕ_0 may be considered as a random variable with Rayleigh distribution,

$$p(\phi_0) = \frac{2\phi_0}{\phi_{\text{DM}}^2} \exp\left(-\frac{\phi_0^2}{\phi_{\text{DM}}^2}\right), \quad (9)$$

where $\phi_{\text{DM}} = \sqrt{2\rho_{\text{DM}}}/m$ is an average amplitude of the dark matter field. The variance of the scalar field amplitude stems from the stochastic nature of velocities of dark matter particles near the Solar system within the standard dark matter halo model, see, e.g., Refs. [4–6]. This model ignores possible nonvirialized dark matter streams [35] and composite dark matter structures such as boson stars [36] or topological defects [37], which are to be studied separately. In the present case, in Eq. (8) one may turn from averaging over time to the averaging over the amplitude ϕ_0 with the distribution (9). Then, the energy level shift (6) has random fluctuations with exponential distribution. As a result, $k = 1$ and Eq. (8) allows us to identify a theoretically calculated atomic energy level shift with experimentally measured energy variance of this level,

$$\sigma = \bar{E}. \quad (10)$$

This method is broadband as it does not require performing Fourier analysis of the data. The principal assumption in this approach is that the measurement time t_1 satisfies the conditions (7). Given that $T = \pi/m$, we can convert these conditions to the constraints on the scalar field mass if the time t_1 is experimentally fixed,

$$\pi/t_1 \ll m \ll 10^6 \pi/t_1. \quad (11)$$

Thus, an experiment measuring fluctuations of frequencies of atomic clocks during the time t_1 is suitable for

searches of the axion and scalar dark matter with particle mass in the range (11).

This approach may be efficient when axion or scalar mass is not too small. For instance, assume that the averaging time is $t_1 > 10^{-6}$ s, then the coherence time obeys $\tau > t_1 > 10^{-6}$ s, and the oscillation period is $T \sim 10^{-6}\tau > 10^{-12}$ s. Assuming also that the total measurement time is about one day, we have $\tau < t \sim 10^5$ s and obtain the range of dark matter particle masses 10^{-13} eV $< m < 0.01$ eV. The QCD axion with the mass $m \sim 10^{-5}$ eV falls within this region.

Note that a similar proposal of exploring fluctuations of the dark matter amplitude has been recently presented in Ref. [25]. The novel feature of the present work is the idea of using experimental value of the variance to find the limits on the axion decay constant. This idea will be illustrated by the following two examples.

III. LIMITS FROM ATOMIC CLOCKS EXPERIMENTS

Measurements of time dependence of the ratio of frequencies of Rb and Cs hyperfine transitions were implemented in the work [11]. Using calculations in Refs. [21, 27], we find this ratio in the form

$$\frac{\delta(\nu_{\text{Rb}}/\nu_{\text{Cs}})}{\nu_{\text{Rb}}/\nu_{\text{Cs}}} = 10^{-16} \frac{(1 + \cos(2mt))}{m_{15}^2 f_{10}^2} \frac{\phi_0^2}{\phi_{\text{DM}}^2}, \quad (12)$$

where $m_{15} \equiv m/(10^{-15}$ eV), $f_{10} \equiv f_a/(10^{10}$ GeV), m and f_a are the axion mass and interaction constant. The reported standard deviation in measurements of variation of the ratio of frequencies is $\sigma = 3 \times 10^{-15}$ [11]. The averaging time in this experiment $t_1 = 864$ s allows us to obtain limits for the axion mass in the range 2.4×10^{-18} eV $< m < 2.4 \times 10^{-12}$ eV:

$$f_a > 1.8 \times 10^9 \text{ GeV} \left(\frac{10^{-15} \text{ eV}}{m} \right). \quad (13)$$

The corresponding exclusion region is shown in Fig. 1 by the blue area. Although this limit is still many orders in magnitude weaker than the QCD axion line, Eq. (13) gives a new constraint on the axion coupling f_a for axion masses in the range 2×10^{-17} eV $\lesssim m \lesssim 10^{-13}$ eV which is not covered by other lab-based experiments. Note that in presenting these constraints in Fig. 1 we assume that the parameters f_a and m are independent while they are related as $f_a m \approx f_\pi m_\pi$ for the canonical QCD axion.

Similar limit may be obtained from the comparison of the hydrogen hyperfine transition with the silicon cavity eigenmode performed in Ref. [13]. Dependence of the ratio of corresponding frequencies on the fundamental constants has been obtained in Refs. [21, 22]

$$\frac{\nu_{\text{H}}}{\nu_{\text{Si}}} \propto \alpha^3 R(Z\alpha) \frac{m_e}{m_p} g_p, \quad (14)$$

where m_e and m_p are electron and proton masses, respectively, g_p is the proton magnetic g -factor, α is the fine

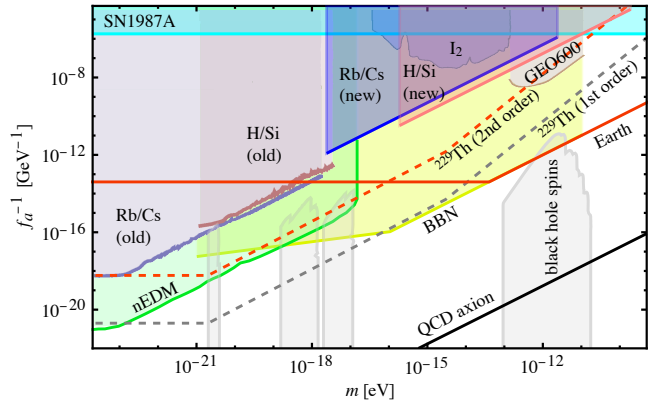


FIG. 1. New limits on the axion coupling constant f_a from re-purposing the results of the Rb/Cs atomic clocks experiments [11] (blue shaded region) and H/Si cavity experiment [13] (pink shaded region). These limits are compared with the earlier found constraints from the same experiments obtained in Ref. [27] (gray shaded regions labeled as Rb/Cs (old) and H/Si (old) respectively). Dashed red line represents projected sensitivity of ^{229}Th nuclear clocks to the axion field through the second-order energy shift in the perturbation theory, and dashed gray line corresponds to the first-order perturbation theory correction found in Ref. [27]. The black straight line in the right bottom corner is the QCD axion benchmark line with $f_a m \approx f_\pi m_\pi$. For comparison, we included also the constraints from I_2 molecular spectroscopy experiment [39], GEO 600 gravitational detector [40], nuclear spin precession experiment (nEDM) [41], big bang nucleosynthesis (BBN) [42], supernova explosions (SN1987A) [43] and analysis of black hole spins [44, 45]. The red solid line labeled “Earth” represents constraints due to possible axion emissions from the Earth [46].

structure constant, Z is the nuclear charge and $R(Z\alpha)$ is the relativistic factor which for hydrogen and silicon is close to 1. Using calculations presented in Ref. [27] we obtain

$$\frac{\delta(\nu_{\text{H}}/\nu_{\text{Si}})}{\nu_{\text{H}}/\nu_{\text{Si}}} = 10^{-15} \frac{(1 + \cos(2mt))}{m_{15}^2 f_{10}^2} \frac{\phi_0^2}{\phi_{\text{DM}}^2}. \quad (15)$$

Equating this frequency variation to the dispersion of the experimental data in Ref. [13], $\sigma \approx 3 \times 10^{-15}$, we find the limit on the axion decay constant:

$$f_a > 5.8 \times 10^9 \text{ GeV} \left(\frac{10^{-15} \text{ eV}}{m} \right). \quad (16)$$

Although this constraint is comparable with that in Eq. (13), it applies to a slightly different axion mass range 1.9×10^{-16} eV $< m < 1.9 \times 10^{-10}$ eV which corresponds to the integration time $t_1 = 10.7$ s [38]. The corresponding exclusion region is shown in Fig. 1 by a pink area.

This effect may also be measured in molecules where vibrational and rotational transitions are sensitive to variation of nucleon mass, see, e.g., Ref. [27, 39]. In fact, variance in the fluctuations of energy levels was measured in numerous papers searching for the linear drift of the

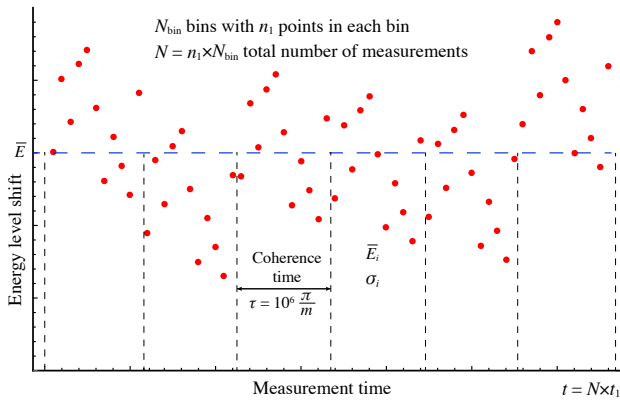


FIG. 2. Illustration of binning of measurements of atomic energy level shift with atomic clocks to determine the axion mass. Total measurement time $t = Nt_1$ is divided into time intervals equal to the duration of the scalar field coherence time $\tau = 10^6\pi/m$ such that each bin contains results of n_1 measurements. Energy shift measurements in each bin are distributed quasi Gaussian with mean \bar{E}_i and dispersion σ_i . The energy shifts \bar{E}_i in different bins follow the exponential distribution if the bin size corresponds to the dark matter coherence time.

fundamental constants. This variance is linked to statistical error of the drift measurements.

IV. POSSIBLE SIGNATURE OF THE AXION SIGNAL

The relation (10) has been used to extract limits on the axion coupling f_a from measured fluctuations of relative frequencies of atomic clocks. This consideration, however, does not allow one to identify the signal of axion dark matter if it is present in the data.

In Refs. [25, 26] it was proposed that the axion field may manifest itself in correlated fluctuations of energy shifts in a network of atomic clocks or magnetometers. Such a correlation is possible if the detectors in a network are separated by a distance not exceeding the dark matter particle correlation lengths. Here we show that, in principle, it is possible to find a signature of the ultra-light axion dark matter even with a single atomic clock measuring relative atomic energy level shift within a sufficiently long period of time. The main idea is that fluctuations of atomic energy levels due to the axion or scalar field dark matter are governed by a different statistical distribution as compared with ordinary Gaussian noise.

Assume that the mass m of the axion (or scalar) field ϕ is known. As is argued above, the amplitude ϕ_0 of this field fluctuates with a typical coherence time $\tau = 10^6 T = 10^6\pi/m$. This means that the mean atomic energy level shift (6) is nearly constant during one coherence time period, but the values \bar{E}_i in different time intervals τ have stochastic nature with exponential distribution. An important feature of this distribution is that

the dispersion of the energy shifts \bar{E}_i is equal to the total mean energy shift (10). Another important feature of this distribution is the presence of non-vanishing higher statistical moments such as skewness S and kurtosis K :

$$S \equiv \frac{(\bar{E}_i - \bar{E})^3}{\sigma^3} = 2, \quad K \equiv \frac{(\bar{E}_i - \bar{E})^4}{\sigma^4} = 9. \quad (17)$$

Thus, checking the experimental data of atomic energy level shifts for non-vanishing values of the skewness and kurtosis may help identify if these fluctuations are caused by variations of the amplitude of the axion dark matter.

The problem is, however, that the mass of the axion field and, hence, the coherence time are not known. The integration time t_1 of one frequency shift measurement may be either longer or shorter than this coherence time. In the latter case, we can write $\tau = n_1 t_1$, where n_1 is the (unknown) mean number of energy shift measurements per dark matter particle coherence time τ .

We may assume that fluctuations of energy shift measurements within one coherence time interval correspond to white noise in the detector rather than the variation of the scalar field amplitude. Thus, these fluctuations should be governed by the normal Gaussian distribution with mean energy shift \bar{E}_i and dispersion σ_i . Recall that the normal distribution, in contrast with the exponential distribution, has vanishing odd statistical moments and kurtosis $K = 3$ that is strongly different from the exponential distribution assumed for the energy shifts caused by the axion field (17).

We propose the following procedure for searching for the axion mass with the use of data of measurements of atomic energy level shifts in atomic clock experiments. The total number of measurements N is divided into N_{bin} bins with n_1 data points in each bin as in Fig. 2. The energy level shift measurements within each bin are averaged yielding \bar{E}_i , $i = 1, 2, \dots, N_{\text{bin}}$. If the number of points per bin is such that $n_1 t_1 = \tau$, the values \bar{E}_i should (approximately) follow the exponential distribution and, hence, satisfy the conditions (10) and (17). The number of points per bin n_1 may be varied in the interval $1 < n_1 \leq N/2$ searching for these conditions. If such number n_1 is found, the axion mass is expressed as

$$m \approx \frac{10^6\pi}{n_1 t_1}. \quad (18)$$

This procedure may help find an approximate value of the axion mass, which should serve as a motivation for further experiments to search for the axion particle with the mass near this value. It is reminiscent of the stacking procedure proposed in Ref. [47] for optimizing the storage and statistical analysis of experimental data.

For an illustration of this procedure we perform a Monte-Carlo simulation of experimental data with $N_{\text{bin}} = 992$ pseudorandom values of \bar{E}_i with exponential distribution. We choose these values such that $\bar{E} = \sigma = 25$ in some units. For each \bar{E}_i we generate pseudorandomly $n_1 = 193$ points E_{ik} with mean value

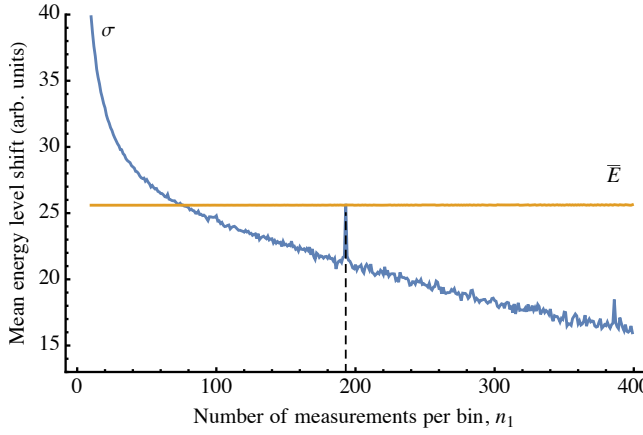


FIG. 3. Simulation of the binning procedure for finding the axion mass. Horizontal axis measures the number of points per bin out of total 992×193 simulated energy shift measurements. Vertical axis corresponds to mean atomic energy level shift \bar{E} in arbitrary units. Blue curve represents the standard deviation σ calculated for mean energy shifts \bar{E}_i in each bin. This curve has a peak near $n_1 = \tau/t_1$ (dashed line), where τ is the coherence time and t_1 is the time of one measurement. This peak indicates that the mass of the axion dark matter particle is close to the value $m \approx 10^6 \pi / (n_1 t_1)$.

\bar{E}_i and standard deviation $\sigma = 100$ in the same units. For fixed i , the variance of E_{ik} represents the Gaussian noise in the detector, while the variance of \bar{E}_i originates from fluctuations of the scalar field amplitude ϕ_0 . The total of 992×193 points represent the mock data set of an experiment measuring the atomic energy level shift.

Assume now that the axion dark matter coherence time is not known, and it should be determined from the given mock data set. To find it, we divide the data set into N_{bin} bins with n_1 points in each bin, as in Fig. 2. In each bin, the energy shifts are averaged, and values \bar{E}_i are found, $i = 1, 2, \dots, N_{\text{bin}}$. Next, the mean \bar{E} and standard deviation σ are calculated using these \bar{E}_i . This calculation of \bar{E} and σ should be repeated for different values of the bin width n_1 in the range $10 \leq n_1 \leq 400$ in the present case. For the mock data set under consideration, the values of \bar{E} and σ as functions of n_1 are plotted in Fig. 3. In this figure, the value of the standard deviation σ decreases quasi monotonically with n_1 , except for one point $n_1 = 193$ where $\sigma \approx \bar{E}$. Given this value of n_1 , the axion mass is estimated with Eq. (18).

The above simulation of the energy level shift qualitatively demonstrates the procedure for axion mass determination. This procedure may be applied when the noise in the detector is comparable with the expected energy level shift due to the axion dark matter; otherwise, if the noise is too high, the axion signal is totally washed out and the axion mass may not be found. However, if in a real experimental data a similar behaviour is observed, this would be a strong indication that variations of frequencies of atomic clocks are caused by fluctuations of the amplitude of the axion dark matter. It is very

tempting to apply this procedure to the real data sets of experiments reported in Refs. [10–16].

V. SECOND-ORDER PERTURBATION THEORY CORRECTION TO ENERGY LEVELS SHIFT DUE TO LINEAR PSEUDOSCALAR INTERACTION

Standard model spinor fields ψ , photon $F_{\mu\nu}$ and gluon $G_{\mu\nu}^l$ fields can have the following interaction vertices with a pseudoscalar field ϕ :

$$V = \frac{C_f}{f_a} \partial_\mu \phi \bar{\psi} \gamma_5 \gamma^\mu \psi + C_\gamma \frac{\phi}{f_a} \tilde{F}^{\mu\nu} F_{\mu\nu} + C_g \frac{\phi}{f_a} \tilde{G}^{l\mu\nu} G_{\mu\nu}^l. \quad (19)$$

Here C_f , C_γ and C_g are some dimensionless constants which are of order $O(1)$ for the QCD axion model, but are arbitrary for the general pseudoscalar (axion-like) particle. In particular, the last term in Eq. (19) reduces to the QCD θ -term (3) upon the substitution $C_g = g^2/(32\pi^2)$, or

$$\theta = \frac{32\pi^2 C_g \phi}{g^2 f_a}. \quad (20)$$

In atoms and molecules, the interaction (19) cannot produce energy levels shifts in the first order of perturbation theory because the pseudoscalar field mixes the states of opposite parity if one neglects a small axion momentum corresponding to virialized dark matter particles in the standard dark matter halo model. Thus, non-trivial corrections to the energy levels E_n start from the second order in the perturbation theory

$$E^{(2)} = \sum_{n \neq 0} \frac{\langle 0|V|n\rangle \langle n|V|0\rangle}{E_0 - E_n}. \quad (21)$$

The second-order energy corrections may be useful for studying variance of fluctuations of the energy shift averaged over the field oscillations. Such corrections may be significant in the cases of small energy denominators $E_0 - E_n$ in Eq. (21) which is the case of close metastable states in Dy atom, polar molecules with rotational doublets, close levels in nuclear clock based on ^{229}Th . In Dy atom and molecules, the energy interval $E_0 - E_n$ may be reduced to zero by application of magnetic field. Near the level crossing the interval between the levels becomes linear in the perturbation, $|E_n - E_0| = 2|\langle 0|V|n\rangle|$. However, level widths and time-dependent perturbation V make the problem more complicated. We leave this problem for future study.

The second-order energy correction (21) is quadratic in the pseudoscalar field amplitude, $E^{(2)} \propto \phi_0^2$. Therefore, it is interesting to compare this second-order energy level shift with the effect of θ^2 in pion mass (4) discussed in Sec. II. Note that these two contributions to the energy level shift are produced by two independent mechanisms,

although both originate from the same underlying axion-gluon interaction (3). Below we estimate the second-order energy level shift in ^{229}Th nucleus caused by CP -violating pion-nucleon interaction $\sim \theta\pi\bar{N}N$ which was derived in Ref. [48] where neutron EDM due to QCD θ -vacuum was calculated.

Consider, for example, the second-order contribution to the energy shift of the low-lying level $E \equiv \hbar\omega = 8.3$ eV of the nuclear clock transition in ^{229}Th [49]. This shift may be produced by P, T -violating nuclear forces with non-relativistic potential of the general form [50]:

$$V = \xi \vec{\sigma} \nabla V_s. \quad (22)$$

Here ξ is a coupling constant, $\vec{\sigma}$ are the Pauli matrices corresponding to the spin of the nucleon and V_s is the average nucleon-nucleus potential due to the strong interaction.

In this paper, we consider a simple model where V_s is given by an oscillator-type potential,

$$V_s = V_0(r^2/R^2 - 1), \quad (23)$$

with $V_0 \simeq 50$ MeV and the nuclear radius R . This potential vanishes on the boundary of the nucleus at $r = R$, and is negative inside the nucleus. Although this potential represents a crude nuclear model, it allows us to estimate analytically the second-order perturbative correction to the energy level shift of an isomeric state in ^{229}Th . More accurate and sophisticated nuclear models would require numerical methods which are beyond the scope of this paper.

In Ref. [50] the constant ξ was expressed via a dimensionless coupling η , $\xi = -2 \times 10^{-21} \eta \text{ cm}$, which was related with the QCD vacuum angle θ in Ref. [51–53]: $\eta = 4.4 \times 10^5 \theta$. Indeed, the P, T -odd nuclear force (22) is dominated by the π_0 meson exchange [52], while the coupling constants of P, T -odd pion-nucleon interaction were expressed via θ in the classic paper [48]. Making use of Eq. (20), we express ξ via C_g/f_a :

$$\xi = -8.8 \times 10^{-16} \frac{32\pi^2 C_g \phi}{g^2 f_a} \text{ cm}. \quad (24)$$

Thus, the CP -odd potential (22) is first-order in the axion field $\phi = \theta f_a$, and the corresponding second-order energy correction (21) may be cast in the form

$$E^{(2)} = \langle \delta\psi | V | \psi \rangle, \quad (25)$$

where

$$|\delta\psi\rangle = \sum_{n \neq 0} \frac{|n\rangle \langle n| V | \psi \rangle}{E_0 - E_n} \quad (26)$$

is the first-order correction to the wave function ψ . In Ref. [50] this correction was found in the following simple form

$$\delta\psi = \xi \vec{\sigma} \nabla \psi. \quad (27)$$

Substituting this function into Eq. (25), integrating by parts and using commutation identities of Pauli matrices we find

$$E^{(2)} = -3 \frac{\xi^2 V_0}{R^2} - 4 \frac{\xi^2 V_0}{R^2} \langle \vec{l} \cdot \vec{s} \rangle, \quad (28)$$

where \vec{l} and \vec{s} are the nuclear orbital momentum and spin operators, respectively.

Remember that the lowest transition frequency in ^{229}Th is given by the difference between the energies of excited $3/2^+$ [633] and the ground $5/2^+$ [631] nuclear states, $\hbar\omega = E_{3/2^+} - E_{5/2^+}$. Eq. (28) allows us to find the frequency shift of this transition due to P, T -odd hadronic interaction (22),

$$\begin{aligned} \hbar\delta\omega &= -4 \frac{V_0 \xi^2}{R^2} \left(\langle \vec{l} \cdot \vec{s} \rangle_{3/2^+} - \langle \vec{l} \cdot \vec{s} \rangle_{5/2^+} \right) \\ &= -8 \frac{V_0 \xi^2}{R^2}, \end{aligned} \quad (29)$$

where we made use of the identity $\langle \vec{l} \cdot \vec{s} \rangle_{3/2^+} - \langle \vec{l} \cdot \vec{s} \rangle_{5/2^+} = 2$ [31].

The nuclear charge radius of ^{229}Th is $R \approx 7.43$ fm [54]. Substituting this value into Eq. (29) we find the relative frequency shift

$$\delta\omega/\omega \approx -68\theta^2. \quad (30)$$

This result may be compared with the first-order energy shift due to the pion mass variation found in Ref. [27] (using the calculation of the dependence of nuclear energy levels on pion mass from Ref. [31]): $E^{(1)}/E = 2 \times 10^5 \delta m_\pi^2/m_\pi^2 \approx 2 \times 10^4 \theta^2$. Thus, the second-order energy shift (30) is about 300 times smaller than the first-order contribution from pion mass θ -dependence. This allows us to find the limits on the axion constant f_a by re-scaling the corresponding limits from Ref. [27]. This limit is represented in Fig. 1 by the dashed line. We stress that the variation of frequency of nuclear clock considered in this section originates from the term $\cos(2\omega t)$ in ϕ^2 rather than from fluctuations of the (pseudo)scalar field amplitude.

VI. SUMMARY

In this paper, we found two new effects in the QCD axion model which contribute to variations of fundamental constants.

The first effect appears from quadratic axion-nucleon interaction (1) originating from the quadratic dependence of the pion mass on the axion (4). This effect may be observed via variations of frequencies of atomic clocks due to fluctuations of the (pseudo)scalar field amplitude. We show that these variations of frequencies may be identified with variance of measured fluctuations of transition frequencies in the atomic clocks, see Eq. (10). This allows one to explore the region of QCD axion masses satisfying Eq. (11). By re-purposing correspondingly the

results of the experiments [11] and [13] we found new laboratory limits on the axion decay constant f_a in the range 2×10^{-17} eV $\lesssim m \lesssim 10^{-13}$ eV. We propose also a procedure which, in principle, could help find signatures of the axion signal in the energy level shift measurements in atomic clock experiments.

The other effect originates from the second-order perturbative correction to the energy level shift due to linear-in- ϕ interaction. Since this effect is expected to be small, it may manifest itself only in extremely accurate frequency measurements with future technology based on nuclear clocks. We estimated this shift for the low-energy nuclear transition in ^{229}Th and found the projected lim-

its from the expected sensitivity of such nuclear clocks, see Fig. 1.

Acknowledgements.— We are indebted to the Referee for pointing out that the Rayleigh distribution for the axion field amplitude results in non-trivial values of higher statistical moments (17) and for proposing the idea of binning procedure for searches of possible signatures of the axion dark matter in atomic clock experiments. We are grateful also to Dmitry Budker and Yevgeny Stadnik for informing us about Ref. [25] and to Melina Filzinger and Nils Huntemann for valuable comments. The work was supported by the Australian Research Council Grants No. DP230101058 and DP200100150.

[1] J. Preskill, M. B. Wise, and F. Wilczek, *Phys. Lett. B* **120**, 127 (1983).

[2] L. Abbott and P. Sikivie, *Phys. Lett. B* **120**, 133 (1983).

[3] M. Dine and W. Fischler, *Phys. Lett. B* **120**, 137 (1983).

[4] A. K. Drukier, K. Freese, and D. N. Spergel, *Phys. Rev. D* **33**, 3495 (1986).

[5] A. Pillepich, M. Kuhlen, J. Guedes, and P. Madau, *Astrophys. J.* **784**, 161 (2014).

[6] N. W. Evans, C. A. J. O'Hare, and C. McCabe, *Phys. Rev. D* **99**, 023012 (2019).

[7] A. Arvanitaki, J. Huang, and K. Van Tilburg, *Phys. Rev. D* **91**, 015015 (2015).

[8] Y. V. Stadnik and V. V. Flambaum, *Phys. Rev. Lett.* **115**, 201301 (2015).

[9] Y. V. Stadnik and V. V. Flambaum, *Phys. Rev. A* **94**, 022111 (2016).

[10] K. Van Tilburg, N. Leefer, L. Bougas, and D. Budker, *Phys. Rev. Lett.* **115**, 011802 (2015).

[11] A. Hees, J. Guéna, M. Abgrall, S. Bize, and P. Wolf, *Phys. Rev. Lett.* **117**, 061301 (2016).

[12] T. Kobayashi, A. Takamizawa, D. Akamatsu, A. Kawasaki, A. Nishiyama, K. Hosaka, Y. Hisai, M. Wada, H. Inaba, T. Tanabe, and M. Yasuda, *Phys. Rev. Lett.* **129**, 241301 (2022).

[13] C. J. Kennedy *et al.*, *Phys. Rev. Lett.* **125**, 201302 (2020).

[14] O. Tretiak *et al.*, *Phys. Rev. Lett.* **129**, 031301 (2022).

[15] A. Banerjee, D. Budker, M. Filzinger, N. Huntemann, G. Paz, G. Perez, S. Porsev, and M. Safronova, Oscillating nuclear charge radii as sensors for ultralight dark matter (2023), arXiv:2301.10784 [hep-ph].

[16] M. Filzinger, S. Dörscher, R. Lange, J. Klose, M. Steinel, E. Benkler, E. Peik, C. Lisdat, and N. Huntemann, *Phys. Rev. Lett.* **130**, 253001 (2023).

[17] N. Sherrill *et al.*, Analysis of atomic-clock data to constrain variations of fundamental constants (2023), arXiv:2302.04565 [physics.atom-ph].

[18] V. A. Dzuba, V. V. Flambaum, and J. K. Webb, *Phys. Rev. Lett.* **82**, 888 (1999).

[19] V. A. Dzuba, V. V. Flambaum, and J. K. Webb, *Phys. Rev. A* **59**, 230 (1999).

[20] V. V. Flambaum and V. A. Dzuba, *Can. J. Phys.* **87**, 25 (2009).

[21] V. V. Flambaum and A. F. Tedesco, *Phys. Rev. C* **73**, 055501 (2006).

[22] L. F. Paštka, Y. Hao, A. Borschevsky, V. V. Flambaum, and P. Schwerdtfeger, *Phys. Rev. Lett.* **122**, 160801 (2019).

[23] V. V. Flambaum and P. Munro-Laylim, *Phys. Rev. D* **107**, 015004 (2023).

[24] T. Bouley, P. Sørensen, and T.-T. Yu, *JHEP* **03**, 104, arXiv:2211.09826 [hep-ph].

[25] H. Masia-Roig *et al.*, *Phys. Rev. D* **108**, 015003 (2023).

[26] A. Derevianko, *Phys. Rev. A* **97**, 042506 (2018).

[27] H. Kim and G. Perez, Oscillations of atomic energy levels induced by QCD axion dark matter (2022), arXiv:2205.12988 [hep-ph].

[28] L. Ubaldi, *Phys. Rev. D* **81**, 025011 (2010).

[29] V. V. Flambaum, D. B. Leinweber, A. W. Thomas, and R. D. Young, *Phys. Rev. D* **69**, 115006 (2004).

[30] V. V. Flambaum and R. B. Wiringa, *Phys. Rev. C* **76**, 054002 (2007).

[31] V. V. Flambaum and R. B. Wiringa, *Phys. Rev. C* **79**, 034302 (2009).

[32] T. H. Dinh, A. Dunning, V. A. Dzuba, and V. V. Flambaum, *Phys. Rev. A* **79**, 054102 (2009).

[33] G. P. Centers *et al.*, *Nature Commun.* **12**, 7321 (2021).

[34] J. W. Foster, Y. Kahn, R. Nguyen, N. L. Rodd, and B. R. Safdi, *Phys. Rev. D* **103**, 076018 (2021).

[35] J. Diemand, M. Kuhlen, P. Madau, M. Zemp, B. Moore, D. Potter, and J. Stadel, *Nature* **454**, 735 (2008).

[36] J. Eby, C. Kouvaris, N. G. Nielsen, and L. C. R. Wijewardhana, *JHEP* **02**, 028, arXiv:1511.04474 [hep-ph].

[37] M. Pospelov, S. Pustelny, M. P. Ledbetter, D. F. Jackson Kimball, W. Gawlik, and D. Budker, *Phys. Rev. Lett.* **110**, 021803 (2013).

[38] This integration time follows from Ref. [13]: The total measurement time in the H/Si cavity experiment 2826942 s should be divided by 368 data points presented in Fig. 1b in this work, and by a factor 720 which represents the decimation of the original data set. Thus, $t_1 = 2826942$ s / (368 \times 720) \approx 10.7 s.

[39] R. Oswald *et al.*, *Phys. Rev. Lett.* **129**, 031302 (2022).

[40] S. Vermeulen *et al.*, *Nature* **600**, 424–428 (2021).

[41] C. Abel *et al.*, *Phys. Rev. X* **7**, 041034 (2017).

[42] K. Blum, R. T. D’Agnolo, M. Lisanti, and B. R. Safdi, *Phys. Lett. B* **737**, 30 (2014).

[43] G. Lucente, L. Mastrototaro, P. Carenza, L. Di Luzio, M. Giannotti, and A. Mirizzi, *Phys. Rev. D* **105**, 123020 (2022).

- [44] V. M. Mehta, M. Demirtas, C. Long, D. J. E. Marsh, L. Mcallister, and M. J. Stott, Superradiance exclusions in the landscape of type IIB string theory (2020), arXiv:2011.08693 [hep-th].
- [45] M. Baryakhtar, M. Galanis, R. Lasenby, and O. Simon, Phys. Rev. D **103**, 095019 (2021).
- [46] A. Hook and J. Huang, JHEP **06**, 036, arXiv:1708.08464 [hep-ph].
- [47] J. W. Foster, N. L. Rodd, and B. R. Safdi, Phys. Rev. D **97**, 123006 (2018).
- [48] R. Crewther, P. Di Vecchia, G. Veneziano, and E. Witten, Phys. Lett. B **88**, 123 (1979).
- [49] B. Seiferle *et al.*, Nature **573**, 243 (2019).
- [50] V. V. Flambaum, I. B. Khriplovich, and O. P. Sushkov, Sov. Phys. JETP **60**, 873 (1984).
- [51] M. Pospelov and A. Ritz, Annals Phys. **318**, 119 (2005).
- [52] V. V. Flambaum, D. DeMille, and M. G. Kozlov, Phys. Rev. Lett. **113**, 103003 (2014).
- [53] J. de Vries, E. Mereghetti, and A. Walker-Loud, Phys. Rev. C **92**, 045201 (2015).
- [54] I. Angeli and K. Marinova, At. Data Nucl. Data Tables **99**, 69 (2013).